***Available online at*** www.pelagiaresearchlibrary.com

**Pelagia Research Library**

**Advances in Applied Science Research, 2014, 5(1):127-142**

**ISSN: 0976-8610**
**CODEN (USA): AASRFC**

# Dufour and soret effects on steady MHD free convective flow past a vertical porous plate embedded in a porous medium with chemical reaction, radiation heat generation and viscous dissipation

**B. Lavanya and A. Leela Ratnam**

*Department of Applied Mathematics, Sri Padmavathi Mahila Visva Vidyalayam, Tirupathi*

---

**ABSTRACT**

*This paper deals with the effects of heat and mass transfer on two-dimensional steady MHD free convection flow along a vertical porous plate embedded in porous medium in presence of thermal radiation, heat generation, viscous dissipation and chemical reaction under the influence of Dufour and Soret effects. The resulting momentum, energy and concentration equations are then made similar by introducing the usual similarity transformations. These similar equations are then solved numerically by using the shooting method along with fourth – order Runge-Kutta integration scheme. Comparison with previously published work is obtained and good agreement is found. The effects of various parameters on the dimensionless velocity, temperature and concentration profiles as well as the local values of the skin-friction coefficient, Nussel number and Sherwood number are displayed graphically and in tabular form.*

**Keywords**: Free convection flow, Thermal radiation, chemical reaction, MHD, heat generation, viscous dissipation, Dufour and Soret.

---

## INTRODUCTION

Coupled heat and mass transfer by free convective in porous media has been widely studied in the recent years due to its wide applications in engineering as post accidental heat removal in nuclear reactors, solar collectors, drying processes, heat exchangers, geothermal and oil recovery, building construction, etc. A comprehensive review of the studies of convective heat transfer mechanism through porous medium has been made by Nield and Bejan [1]. Hiremath and Patil [2] studied the effect on free convection currents on the oscillatory flow through a porous medium, which is bounded by vertical plane surface of constant temperature. Fluctuating heat and mass transfer on three-dimensional flow through porous medium with variable permeability has been discussed by Sharma et al. [3]. A comprehensive account of the available information in this field is provided in books by Pop and Ingham [4], Ingham and Pop [5], Vafai [6], Vadasz [7], etc.

In recent years, the problems of free convective heat and mass transfer flows through a porous medium under the influence of magnetic field have been attracted the attention of a number of researchers because of their possible applications in many branches of science and technology, such as its applications in transportation cooling of re-entry vehicles and rocker boosters, cross-hatching on ablative surfaces and film vaporization in combustion chambers. Magnetohydrodynamics is currently undergoing a period of great enlargement and differentiation of subject matter. In light of these applications, steady MHD free convective flow past a heated vertical flat plate has been studied by many researchers such as Gupta [8], Lykoudis [9] and Nanda and Mohanty [10]. Chaudhary and

Sharma [11] considered combined heat and mass transfer by laminar mixed convection flow from a vertical surface with induced magnetic field. El-Amin [12] studied the MHD free convection and mass transfer flow in a micropolar fluid over a stationary vertical plate with constant suction. The interest in these new problems generates from their importance in liquid metals, electrolytes and ionized gases. Many researchers have studied MHD free convective heat and mass transfer flow in a porous medium. Some of them are Raptis and Kafoussias [13] investigated heat and mass transfer effects on steady MHD over a porous medium bounded by an infinite vertical porous plate with constant heat flux. Kim [14] found that the effects of heat and mass transfer on MHD micropolar flow over a vertical moving porous plate in a porous medium.

Thermal radiation in fluid dynamics has become a significant branch of the engineering sciences and is an essential aspect of various scenarios in mechanical, aerospace, chemical, environmental, solar power and hazards engineering. For some industrial applications such as glass production and furnace design and in space technology applications such as cosmic flight aerodynamics rocket, propulsion systems, plasma physics and spacecraft re-entry aerothermodynamics which operate at higher temperatures, radiation effects can be significant. The effect of radiation on MHD flow and heat transfer problem has become more important industrially. Singh and Shweta Agarwal [15] studied the Heat transfer in a second grade fluid over an exponentially stretching sheet through porous medium with thermal radiation and elastic deformation under the effect of magnetic field. Makinde and Ogulu [16] studied the effect of thermal radiation on the heat and mass transfer flow of a variable viscosity fluid past a vertical porous plate permeated by a transverse magnetic field. Mohammed Ibrahim et al. [17] found the radiation effects on MHD free convection flow of a micropolar fluid past a stretching surface over a non darcian porous medium.

Combined heat and mass transfer problems in presence of chemical reaction are of importance in many processes and thus have received considerable amount of attention in recent times. In processes such as drying, distribution of temperature and moisture over agricultural field and groves of fruit trees, damage of crops due to freezing, evaporation at the surface of a water body, energy transfer in a wet cooling tower and flow in a desert cooler, heat and mass transfer occur simultaneously. Many practical diffusive operations involve the molecular diffusion of a species in the presence of chemical reaction within or at the boundary. Therefore, the study of heat and mass transfer with chemical reaction is of great practical importance to engineers and scientists. Chemical reactions can be codified as either heterogeneous or homogeneous processes. This depends on whether they occur at an interface or as a single-phase volume reaction. A reaction is said to be of first order, if the rate of reaction is directly proportional to the concentration itself. In many chemical engineering processes, there does occur the chemical reaction between a foreign mass and the fluid in which the plate is moving. In view of heat and mass transfer and chemical reactions numerous and wide-ranging applications in various fields like polymer processing industry in particular in manufacturing process of artificial film and artificial fibers and in some applications of dilute polymer solution. Many researchers have been studied chemical reaction effects on steady MHD flow with combined heat and mass transfer; some of them are Alharbi et al. [18], Gangadhar et al. [19], Ibrahim and Makinde [ 20 ], Eldabe [ 21], Seddeek and Almushigeh [ 22], Mohammed Ibrahim [23], Sudhakar Reddy et al. [24], Kishan N and Srinivas M [25], Anjalidevi and David [26].

The study of heat generation in moving fluids is important as it changes the temperature distribution and the particle deposition rate particularly in nuclear reactor cores, fire and combustion modeling, electronic chips and semi conductor wafers. Heat generation is also important in the context of exothermic or endothermic chemical reaction. Vajravelu and Hadjinicolaou [27] studied the heat transfer characteristics in the laminar boundary layer of a viscous fluid over a stretching sheet with viscous dissipation or frictional heating and internal heat generation. Hossain et al [28] studied problem of the natural convection flow along a vertical wavy surface with uniform surface temperature in the presence of heat generation/absorption. Kesavaiah et.al [29] reported that the effects of the chemical reaction and radiation absorption on unsteady MHD convective heat and mass transfer flow past a semi-infinite vertical permeable moving plate embedded in porous medium with heat source and suction. Mohammed Ibrahim and Bhaskar Reddy [30] investigated heat and mass transfer effects on steady MHD free convective flow along a stretching surface with dissipation, heat generation and radiation.

But in the above mentioned studies, Dufour and Soret terms have been neglected from the energy and concentration equations respectively. It has been found that energy flux can be generated not only by temperature gradient but also by concentration gradient as well. The energy flux caused by concentration gradient is called Dufour effect and the same by temperature gradient is called the Soret effect. These effects are very significant when the temperature and concentration gradient are very high. Anghel et al. [31] studied the Dufour and Soret effects on free convection boundary layer over a vertical surface embedded in a porous medium. Postelnicu [32] analyzed the influence of magnetic field on heat and mass transfer from vertical surfaces in porous media considering Soret and Dufour effects. Alam et al. [33] investigated the Dufour and Soret effects on steady MHD mixed convective and mass transfer flow past a semi-infinite vertical plate. Chamkha and Ben-Nakhi [34] analyzed MHD mixed convection-radiation interaction along a permeable surface immersed in a porous medium in the presence of Soret and Dufour's effects. Many researchers have studied Dufour and Soret effects on free convective heat and mass transfer flow in a porous medium; some of them are M.S. Alam and M.M Rahman [35], Sreedhar Sarma et al [36], Mansour et al. [37], El-Aziz [38], Afify [39], Alam and Ahammad [40].

The aim of this paper is to discuss the Dufour and Soret effects on MHD free convection flow past a vertical porous plate placed in porous medium in the presence of chemical reaction, thermal radiation, viscous dissipation and heat source. The set of governing equations and boundary equation of the problem are transformed into a set of nonlinear ordinary differential equation with assisting of similarity transformations are solved using the shooting method along with fourth order Runge-Kutta integration scheme. The effects of different physical parameters on the velocity, temperature and concentration profiles as well as the local skin-friction coefficient, local Nusselt number and local Sherwood number are presented graphically and in tabular form. To verify the obtained results, we have compared the present numerical results with previous work by Alam and Rahman [35]. The comparison results show a good agreement and we confident that our present numerical results are accurate.

**MATHEMATICAL ANALYSIS**

A steady two-dimensional flow of an incompressible and electrical conducting viscous fluid, along an infinite vertical porous plate embedded in a porous medium is considered. The *x*- axis is taken on the infinite plate, and parallel to the free-stream velocity which is vertical and the *y*- axis is taken normal to the plate. A magnetic field $B_0$ of uniform strength is applied transversely to the direction of the flow. Initially the plate and the fluid are at same temperature $T_\infty$ in a stationary condition with concentration level $C_\infty$ at all points. The plate starts moving impulsively in its own plane with velocity $U_0$, its temperature is raised to $T_w$ and the concentration level at the plate is raised to $C_w$. A homogeneous first order chemical reaction between fluid and the species concentration is considered, in which the rate of chemical reaction is directly proportional to the species concentration. The flow configuration and coordinate system are shown in the Figure 1**.** The fluid is assumed to be slightly conducting, and hence the magnetic field is negligible in comparison with the applied magnetic field. It is further assumed that there is no applied voltage, so that electric field is absent. The fluid is considered to be a gray, absorbing emitting radiation but non-scattering medium and the Rosseland approximation is used to describe the radiative heat flux in the energy equation. It is also assumed that all the fluid properties are constant except that of the influence of the density variation with temperature and concentration in the body force term (Boussinesq's approximation). Then, under the above assumptions, the governing boundary layer equations are

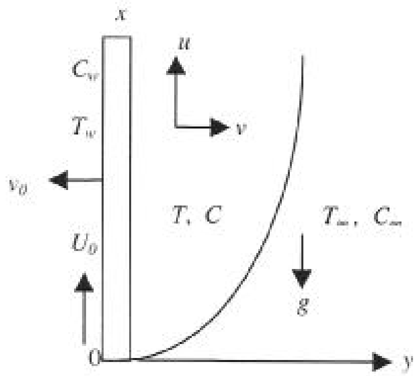


**Fig.1. Flow configuration and coordinate system**

Continuity equation

$$\frac{\partial u}{\partial x}+\frac{\partial v}{\partial y}=0 \qquad (1)$$

Momentum equation

$$u\frac{\partial u}{\partial x}+v\frac{\partial v}{\partial y}=\upsilon\frac{\partial^2 u}{\partial y^2}+g\beta(T-T_\infty)+g\beta^*(C-C_\infty)-\frac{\sigma B_0^2}{\rho}u-\frac{\upsilon}{K}u-\frac{b}{K}u^2 \tag{2}$$

Energy equation

$$u\frac{\partial T}{\partial x}+v\frac{\partial T}{\partial y}=\alpha\frac{\partial^2 T}{\partial y^2}-\frac{1}{\rho c_p}\frac{\partial q_r}{\partial y}+\frac{D_m}{c_s}\frac{k_T}{c_p}\frac{\partial^2 C}{\partial y^2}+\frac{Q_0}{\rho c_p}(T-T_\infty)+\frac{\mu}{\rho c_p}\left(\frac{\partial u}{\partial y}\right)^2 \tag{3}$$

Concentration equation

$$u\frac{\partial C}{\partial x}+v\frac{\partial C}{\partial y}=D_m\frac{\partial^2 C}{\partial y^2}+\frac{D_m k_T}{T_m}\frac{\partial^2 T}{\partial y^2}-kr'(C-C_\infty) \tag{4}$$

where $u,v$ are the Darcian velocities components in the $x$ and $y$ directions respectively, $\upsilon$ is the kinematic viscosity, $g$ is the acceleration due to gravity, $\rho$ is the density, $\mu$ is the dynamic viscosity, $\beta$ is the coefficient of volume expansion with temperature, $\beta^*$ is the volumetric coefficient of expansion with concentration, $b$ is the empirical constant, $T, T_w$ and $T_\infty$ are the temperature of the fluid inside the thermal boundary layer, the plate temperature and the fluid temperature in the free stream, respectively, $C, C_w$ and $C_\infty$ are the corresponding concentrations, $K$ is the Darcy permeability, $\sigma$ is the electric conductivity, $\alpha$ is the thermal diffusivity, $c_p$ is the specific heat at constant pressure, $D_m$ is the coefficient of mass diffusivity, $k_T$ is the thermal diffusion ratio, $c_s$ is the concentration susceptibility, the term $Q_0(T-T_\infty)$ is assumed to be amount of heat generated or absorbed per unit volume and $Q_0$ is a constant, which may take on either positive or negative values, $q_r$ is the radiative heat flux in the $y$-direction, $kr'$ is chemical reaction parameter.

The boundary conditions for velocity, temperature and concentration fields are given by

$$\begin{aligned}&u=U_0,\ v=v_0(x),\ T=T_w,\ C=C_w\ \ at\ \ y=0\\ &u=0,\ v=0,\ T=T_\infty,\ C=C_\infty\ \ \text{as}\ \ y\to\infty\end{aligned} \tag{5}$$

where $U_0$ is the uniform velocity and $v_0(x)$ is the velocity of suction at the plate..

Using the Rosseland approximation for radiation, radiative heat flux is given by Sparrow and Cess [41]

$$q_r=-\frac{4\sigma^*}{3k^*}\frac{\partial T^4}{\partial y} \tag{6}$$

where $\sigma^*$ and $k^*$ are the Stefan-Boltzman constant and the mean absorption coefficient, respectively. We assume that the temperature differences within the flow are such that the term $T^4$ may be expressed as a linear function of temperature. Hence, expending $T^4$ in a Taylor series about $T_\infty$ and neglecting higher order terms we get

$$T^4\equiv 4T_\infty^3T-3T_\infty^4 \tag{7}$$

Using equations (6) and (7) equation (3) becomes

$$u\frac{\partial T}{\partial x}+v\frac{\partial T}{\partial y}=\alpha\frac{\partial^2 T}{\partial y^2}+\frac{16\sigma^*T_\infty^3}{3k^*}\frac{1}{\rho c_p}\frac{\partial^2 T}{\partial y^2}+\frac{D_m}{c_s}\frac{k_T}{c_p}\frac{\partial^2 C}{\partial y^2}+\frac{Q_0}{\rho c_p}(T-T_\infty)+\frac{\mu}{\rho c_p}\left(\frac{\partial u}{\partial y}\right)^2 \tag{8}$$

The equations (2), (4) and (8) are coupled, parabolic and nonlinear partial differential equations and hence analytical solution is not possible. Therefore numerical technique is employed to obtain the required solution. Numerical computations are greatly facilitated by non-dimensionalization of the equations. Proceeding with the analysis, we introduce the following similarity transformations and dimensionless variables which will convert the partial differential equations from two independent variables $(x, y)$ to a system of coupled, non-linear ordinary differential equations in a single variable $(\eta)$ i.e., coordinate normal to the plate.

In order to write the governing equations and the boundary conditions in dimensionless form, the following non-dimensional quantities are introduced.

$$\eta = y\sqrt{\frac{U_0}{2\upsilon x}}, \quad \psi = \sqrt{\upsilon x U_0}\; f(\eta), \quad \theta(\eta) = \frac{T - T_\infty}{T_w - T_\infty}, \quad \phi(\eta) = \frac{C - C_\infty}{C_w - C_\infty} \tag{9}$$

where $f(\eta)$ is the dimensionless stream function and $\psi$ is the dimensional stream function defined in the usual way

$$u = \frac{\partial \psi}{\partial x} \text{ and } v = -\frac{\partial \psi}{\partial y}$$

Clearly the continuity equation (1) is identically satisfied,

Then introducing the relation (9) into equation (1) we obtain

$$u = U_0 f'(\eta) \text{ and } v = \sqrt{\frac{\upsilon U_0}{2x}}\;(\eta f' - f)\,. \tag{10}$$

Further introducing equations (9) and (10) into momentum equation (2), Energy equation (8) and Concentration equation (4) we obtain the following local similarity equations

$$f''' + ff'' + Gr\theta + Gc\phi - Mf' - \frac{1}{Da\,\mathrm{Re}} f' - \frac{Fs}{Da} f'^2 = 0 \tag{11}$$

$$\left(1 + \frac{16}{3R}\right)\theta'' + \Pr f\theta' + \Pr Du\phi'' + \Pr Q\theta + \Pr Ec\left(f''\right)^2 = 0 \tag{12}$$

$$\phi'' + Scf\phi' + ScSr\theta'' - Kr\phi = 0 \tag{13}$$

where

$Gr = \dfrac{g\beta(T_w - T_\infty)2x}{U_0^2}$ is the Grashof number, $Gc = \dfrac{g\beta^*(C_w - C_\infty)2x^2}{\upsilon U_0}$ is mass Grashof number

$M = \dfrac{\sigma B_0^2 2x}{\rho U_0}$ is the magnetic field parameter, $Da = \dfrac{K}{2x^2}$ is the Darcy number, $\mathrm{Re} = \dfrac{U_0 x}{\upsilon}$ is the Reynolds number, $Fs = \dfrac{b}{x}$ is the Forchheimer number, $\Pr = \dfrac{\upsilon}{\alpha}$ is the Prandtl number , $R = \dfrac{k^*\alpha\rho c_p}{\sigma T_\infty^3}$ is the Radiation parameter, $Du = \dfrac{D_m K_T (C_w - C_\infty)}{c_s c_p \upsilon (T_w - T_\infty)}$ is the Dufour number, $Sr = \dfrac{D_m K_T (T_w - T_\infty)}{\upsilon T_m (C_w - C_\infty)}$ is the Soret number, $Ec = \dfrac{U_0^2}{c_p (T_w - T_\infty)}$ is the Eckert number, $Q = \dfrac{Q_0 \upsilon}{\rho c_p U_0^2}$ is the heat generation parameter, $Sc = \dfrac{\upsilon}{D_m}$ is the Schmidt number, $Kr = \dfrac{2Kr' \upsilon x}{D_m U_0}$ is the chemical reaction parameter.

The corresponding boundary conditions are

$$f = f_w,\ f' = 1,\ \theta = 1,\ \phi = 1 \text{ at } \eta = 0,$$
$$f' = 0,\ \theta = 0,\ \phi = 0 \text{ as } \eta \to \infty \tag{14}$$

Where $f_w = -v_0 \sqrt{\dfrac{2x}{\upsilon U_0}}$ is the dimensionless suction velocity and primes denote partial differentiation with respect to the variable $\eta$.

The parameters of engineering interest for the present problem are the skin-friction coefficient, the Nusselt number and the Sherwood number, which are given respectively by the following expressions. Knowing the velocity field the skin-friction at the plate can be obtained, which in non-dimensional form is given by

$$\frac{1}{2} \mathrm{Re}^{\frac{1}{2}} C_f = f''(0) \tag{15}$$

Knowing the temperature field, the rate of heat transfer coefficient can be obtained, which in non-dimensional form, in terms of Nusselt number, is given by

$$Nu\,\mathrm{Re}^{-\frac{1}{2}} = -\theta'(0) \tag{16}$$

Knowing the concentration field, the rate of mass transfer coefficient can be obtained, which in non-dimensional form, in terms of Sherwood number, is given by

$$Sh\,\mathrm{Re}^{-\frac{1}{2}} = -\phi'(0) \tag{17}$$

Where $\mathrm{Re} = \dfrac{U_0 x}{\upsilon}$ is the Reynold is's number.

**Mathematical Solution**

The numerical solutions of the non-linear differential equations (11) – (13) under the boundary conditions (14) have been performed by applying a shooting method along with the fourth order Runge-Kutta method. First of all higher order non-linear differential equations (11) – (13) are converted into simultaneous linear differential equations of first order and they are further transformed into initial value problem by applying the shooting technique. From this process of numerical computation, the skin-friction coefficient, the Nusselt number and Sherwood number which are respectively proportional to $f''(0), -\theta'(0)$ and $-\phi'(0)$ are also sorted out and their numerical values are presented in a tabular form.

## RESULTS AND DISCUSSION

From the numerical computations, dimensionless velocity, temperature and concentration profiles as well as the skin-friction coefficient, Nusselt number and Sherwood number are found for different values of the various physical parameters occurring in the problem. The value of Prandtl number *Pr* is taken to be 0.71 which corresponds to air and the value of Schmidt number *Sc* is chosen 0.22, which represents hydrogen at $25^0$ C and 1 atm. Due to free convection problem positive large values of $Gr = 12$ and $Gc = 6$ are chosen. The value of *Re* is kept 100 and $F_s$ equal to 1.0. The values of Dufour number and Soret number are chosen in such a way that their product is constant provided that the mean temperature $T_m$ is constant as well. However, the values of Darcy number *Da* = 1.0, magnetic field parameter *M* = 1.0, suction parameter $f_w = 0.5$, radiation parameter *R* = 1.0, heat generation parameter *Q* = 1.0, Eckert number $Ec = 0.1$, chemical reaction parameter *Kr* = 0.5 are chosen arbitrarily. The numerical results for velocity, temperature and concentration profiles are displayed in Figs. 2 to 16.

The effect of Grashof number *Gr* on the velocity field is presented in Fig.2. The Grashof number *Gr* signifies the relative effect of the thermal buoyancy force to the viscous hydrodynamic force in the boundary layer. As Grashof number *Gr* increases the velocity of the fluid increases. Fig.3. present velocity profiles in the boundary layer for various values of modified Grashof number *Gc*. The modified Grashof number *Gc* defines the ratio of the species buoyancy force to the viscous hydrodynamic force. As modified Grashof number *Gc* increases the fluid velocity increases.

The effect of Darcy number *Da* on the temperature field is shown in Fig.4. From this figure we observe that velocity increases with the increase of Darcy number *Da*. For large Darcy number porosity of the medium increases, hence fluid flows quickly.

The effect of Reynolds number *Re* on the velocity fields are shown in Fig.5. It is noted that negligible effect of Reynolds number on velocity profiles.

Figs. 6(a) – 6(c) depicts the effect of Forchheimer number *Fs* on the velocity, temperature and concentration profiles. It is observed from Fig. 6(a) that the velocity of the fluid decreases with the increase of Forchheimer number *Fs*. Since Forchheimer number *Fs* represents the inertial drag, thus an increase in the Forchheimer number *Fs* increases the resistance to the flow and so a decrease in the fluid velocity ensues. It is noticed from Fig. 6(b) that temperature of the fluid increases with increase of Forchheimer number *Fs*, since as the fluid is decelerated; energy is dissipated as heat and serves to increase temperature. From Fig. 6(c), it is observed that the concentration of the fluid increases with increase of the Forchheimer number *Fs.*

Fig.7 (a), 7(b) and 7(c) display the velocity, temperature and concentration profiles for different values of magnetic field parameter *M* when the other parameters are fixed. An applied of a magnetic field within boundary layer has produced resistive-type force which known as Lorentz force. This force act to retard the fluid motion along surface and simultaneously increase its temperature and concentration values. Therefore, one can see that the velocity boundary layer thickness decreases with the increase of magnetic field parameter *M* as shown in Fig.7 (a). However, the temperature and concentration increase with the increasing of the magnetic field parameter *M* shown in Fig.7 (b) and Fig.7(c).

Fig.8 (a). Illustrates the velocity profiles for different values of the Prandtl number *Pr*. The numerical results show that the effect of increasing values of Prandtl number results in a decreasing velocity. From Fig.8 (b), it is observed that an increase in the Prandtl number results in a decrease of the thermal boundary layer thickness and in general lower average temperature within the boundary layer. The reason is that smaller values of *Pr* are equivalent to increasing the thermal conductivities, and therefore heat is able to diffuse away from the heated plate more rapidly than for higher values of *Pr*. Hence in the case of smaller Prandtl numbers as the boundary layer is thicker and the rate of heat transfer is reduced.
The effect of the radiation parameter *R* on the velocity and temperature profiles are shown in Figs. 9(a) and 9(b) respectively. Fig.9 (a) shows that velocity profiles decreases with an increase in the radiation parameter *R*. From Fig.9 (b), it is seen that the temperature decreases as the radiation parameter *R* increase. This result qualitatively agrees with expectations, since the effect of radiation is to decrease the rate of energy transport to the fluid, thereby decreasing the temperature of the fluid.

Figs. 10(a) and 10(b) depict the velocity and temperature profiles for different values of the heat generation parameter *Q*. It is noticed that an increase in the heat generation parameter *Q* results in an increase in velocity and temperature within the boundary layer.

Figs. 11(a) and 11(b) show the influence of the Eckert number *Ec*, on the velocity and temperature profiles, respectively. By analyzing these Figs, it is clearly revealed that the effect of Eckert number is to increase both the velocity and temperature distributions in the flow region. This is due to the face that the heat energy is stored in liquid due to the frictional heating. Thus the effect of increasing *Ec* is to enhance the temperature at any point as well as the velocity.

Fig.12 (a), 12(b) and 12(c) show the combination effects of the Dufour and Soret numbers on the fluid velocity, temperature and concentration respectively. The Dufour number *Du* and Soret number *Sr* represent the thermal-diffusion and diffusion-thermal effects in this problem. Fig.12 (a), shows the influences of the Dufour and Soret number on the variations of the fluid velocity. For the case of increasing Dufour number and decreasing Soret number, it is seen that the velocity profiles decreases.

Fig.12(b), illustrate the effects of the Dufour and Soret number on the variations of the fluid temperature. From Fig.12 (b), we observe that an increasing Dufour number and decreasing Soret number, it is seen that the temperature profiles increases. The Dufour term describes the effect of concentration gradients as noted in Equation (12), plays a vital role in assisting the flow and able to increase thermal energy in the boundary layer. This is the evident for the increasing values in the fluid temperature as the Dufour number *Du* increase and the Soret number *Sr* decrease.

In Fig.12(c), as increasing Dufour number *Du* and simultaneously decreasing Soret number *Sr* has implies significant effects on the concentration profiles. The Soret term exemplifies the temperature gradient effects on the variation of concentration as noted in Equation (13). It is observed as the Dufour number increase and Soret number is decrease, the concentration values is found to be decreases.

The influence of Schmidt number *Sc* on the velocity and concentration profiles is plotted in Figs.13 (a) and 13(b) respectively. As the Schmidt number *Sc* increases the concentration decreases. This causes the concentration buoyancy effects to decrease yielding a reduction in the fluid velocity. The reductions in the velocity and concentration profiles are accompanied by simultaneous reductions in the velocity and concentration boundary layers. These behaviors are clear from Figs. 13(a) and 13(b).

The effects of the chemical reaction parameter *Kr* on the velocity and concentration profiles are shown in Figs. 14(a) and 14(b) respectively. As the chemical reaction parameter *Kr* increases the concentration decreases.

The effects of suction parameter $f_w$ on the velocity profiles are shown in Figs.15 (a). It is found from Fig.15 (a) that the velocity profiles decrease monotonically with the increase of suction parameter indicating the usual fact that suction stabilizes the boundary layer growth. The effects of suction parameter on the temperature and concentration field are displayed in Fig.15 (b) and Fig.15(c) respectively. From Fig.15 (b), it is noticed that the temperature decreases with an increase of suction parameter $f_w$. From Fig.15(c), it is observed that the concentration decreases with an increase of suction parameter $f_w$.

The variation of skin-friction coefficient, heat and mass transfer coefficient with radiation parameter *R* and magnetic field parameter *M* are shown in Figs.16 (a), 16(b) and 16(c) respectively. We observe that the effect of increasing *M* is the decrease in the decrease in the heat and mass transfer and skin friction coefficient. On the other hand, the magnitude of the heat and mass transfer increases while that of skin friction coefficient decreases as radiation parameter *R* increases.

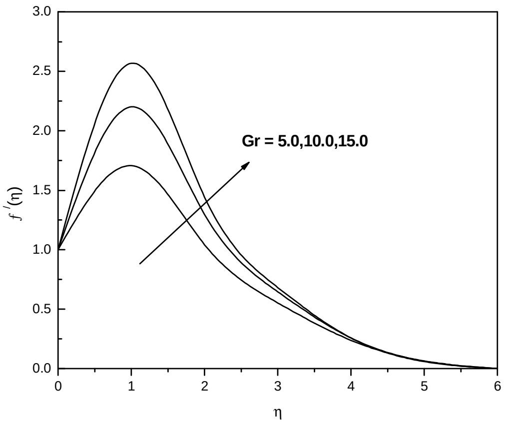


**Fig.2. Velocity profiles for different values of *Gr***

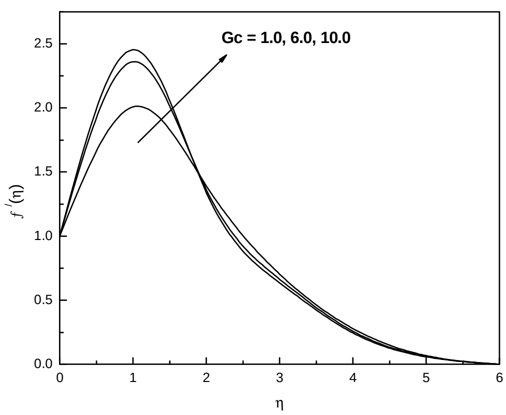


**Fig.3. Velocity profiles for different values of *Gc***

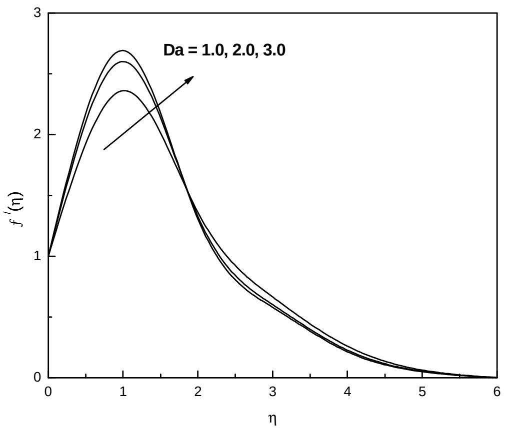


**Fig.4. Velocity profiles for different values of *Da***

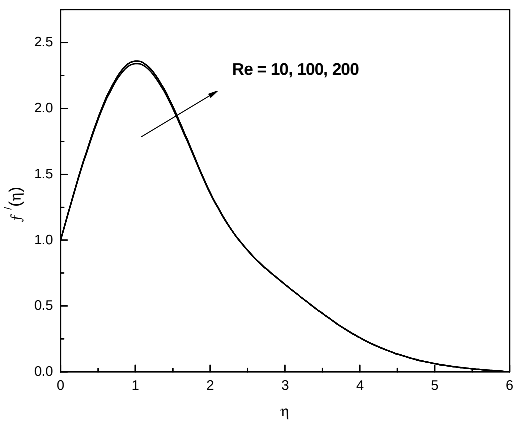


**Fig.5. Velocity profiles for different values of *Re***

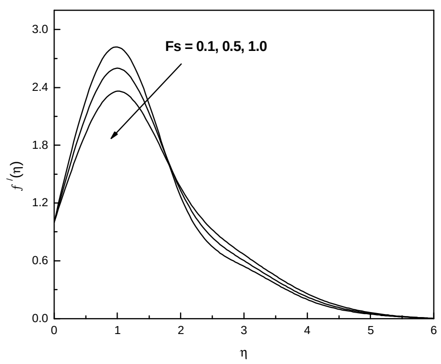


**Fig.6(a). Velocity profiles for different values of *Fs***

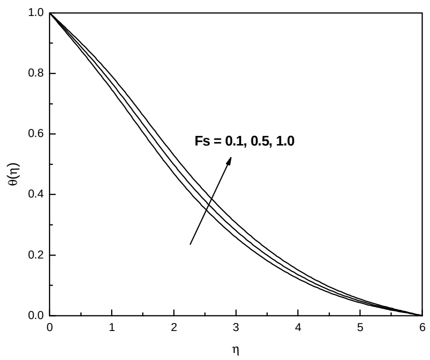


**Fig.6(b). Temperature profiles for different values of *Fs***

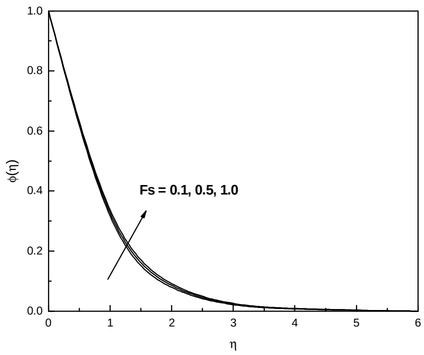


**Fig.6(c). Concentration profiles for different values of *Fs***

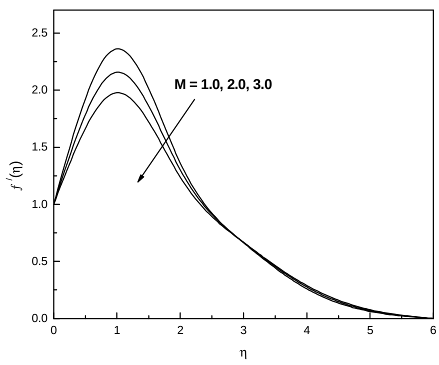


**Fig.7 (a). Velocity profiles for different values of *M***

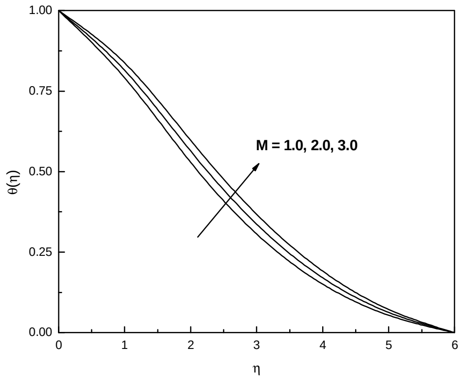


**Fig.7 (b). Temperature profiles for different values of *M***

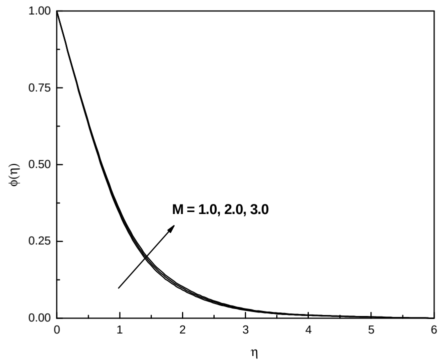


**Fig.7(c). Concentration profiles for different values of *M***

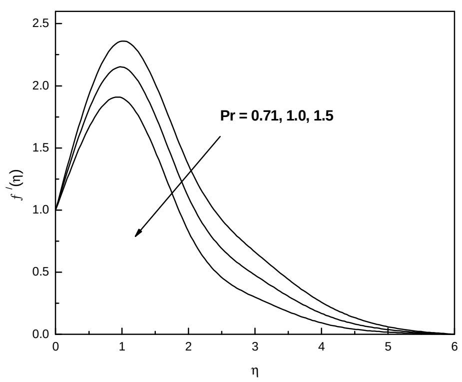


**Fig.8 (a). Velocity profiles for different values of *Pr***

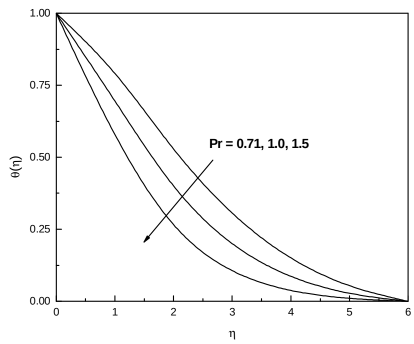


**Fig.8 (b). Temperature profiles for different values of *Pr***

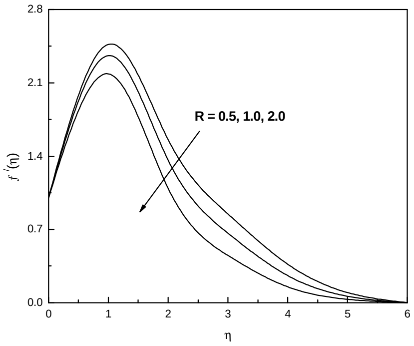


Fig.9 (a). Velocity profiles for different values of *R*

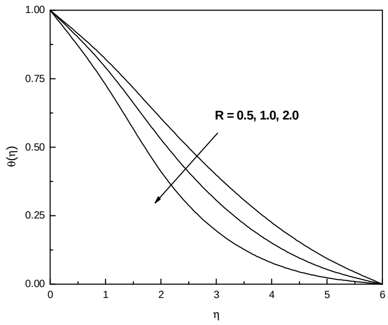


Fig.9 (b). Temperature profiles for different values of *R*

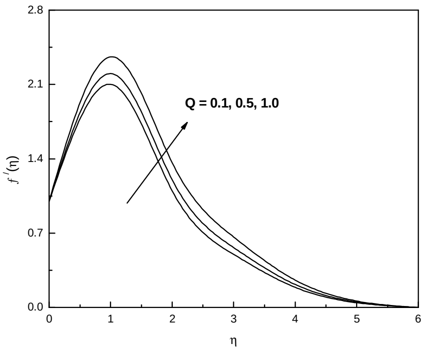


Fig.10 (a). Velocity profiles for different values of *Q*

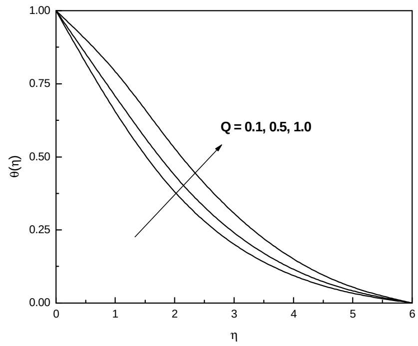


Fig.10 (b). Temperature profiles for different values of *Q*

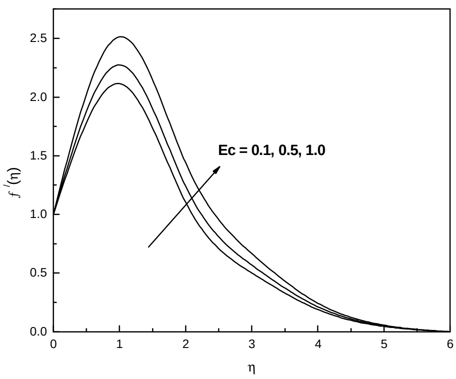


Fig.11 (a). Velocity profiles for different values of *Ec*

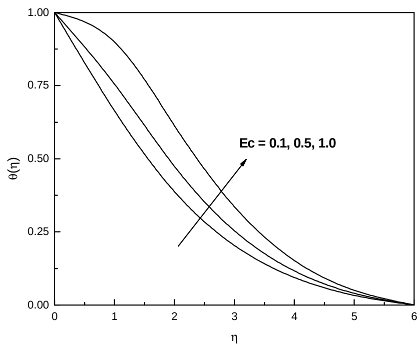


Fig.11 (b). temperature profiles for different values of *Ec*

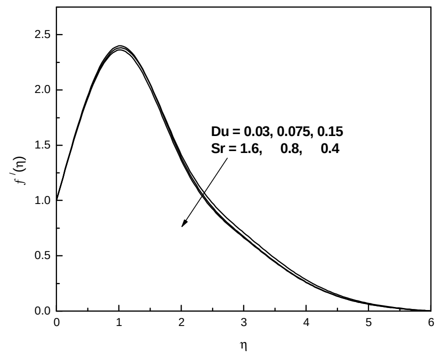


Fig.12 (a). Velocity profiles for different values of *Sr* and *Du*

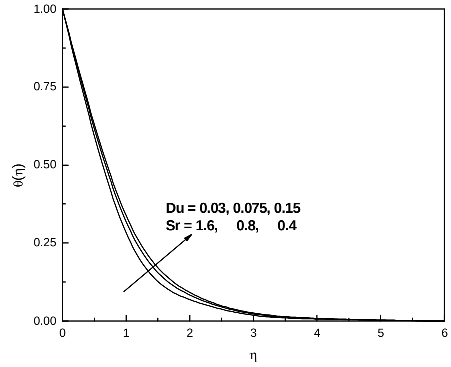


Fig.12 (b). Temperature profiles for different values of *Sr* and *Du*

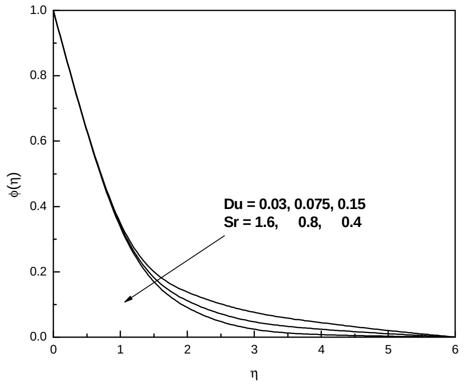


Fig.12(c). Concentration profiles for different values of *Sr* and *Du*

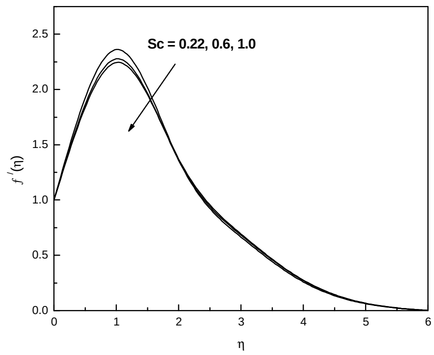


Fig.13 (a). Velocity profiles for different values of *Sc*

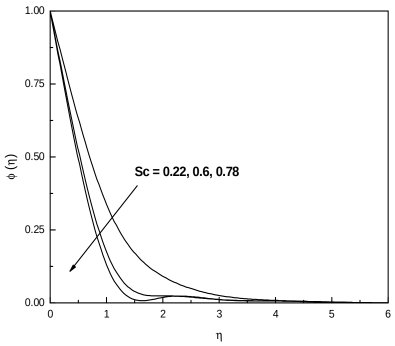


Fig.13(b). Concentration profiles for different values of *Sc*

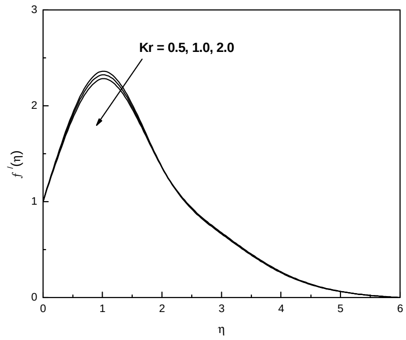


Fig.14 (a). Velocity profiles for different values of *Kr*

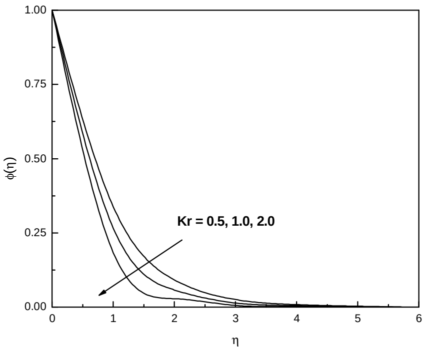


**Fig.14 (b). Concentration profiles for different values of *Kr***

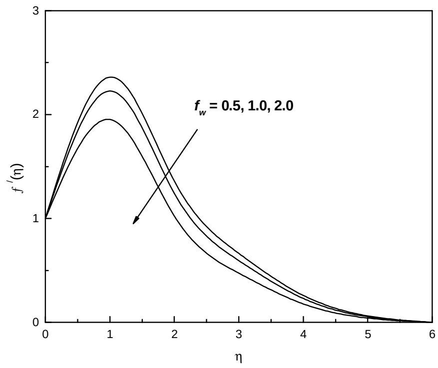


**Fig.15(a).Velocity profiles for different values of** $f_w$

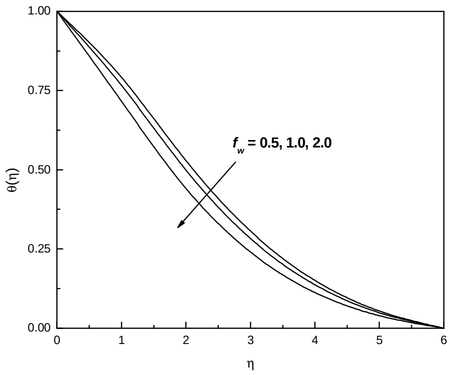


**Fig.15 (b). temperature profiles for different values of** $f_w$

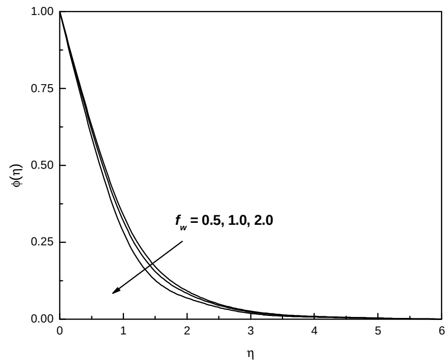


**Fig.15(c). Concentration profiles for different values of** $f_w$

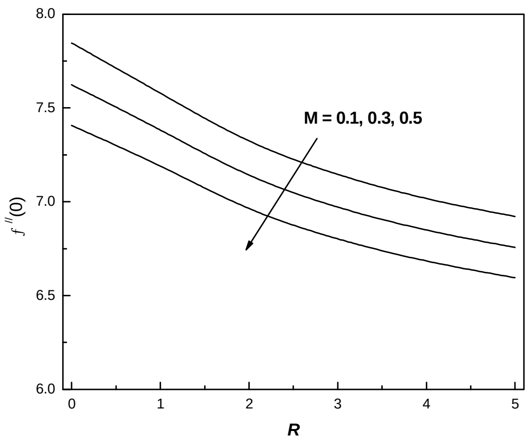


**Fig.16 (a). Variation of** $f''(0)$ **with *R* and *M***

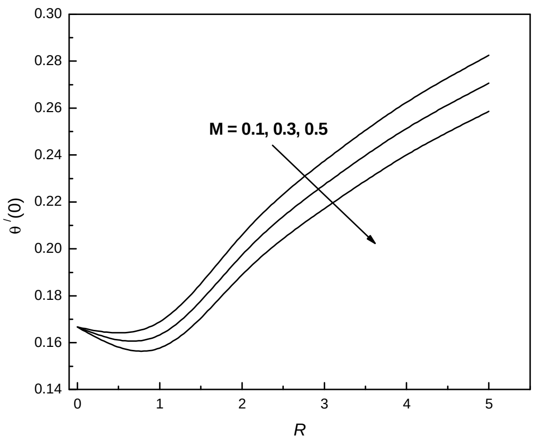


**Fig.16 (b). Variation of the heat flux** $-\theta'(0)$ **with *R* and *M***

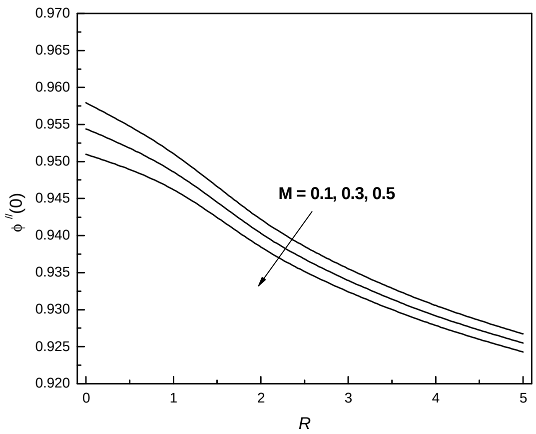


**Fig.16(c). Variation of the mass flux $-\phi'(0)$ with *R* and *M***

Table 1 shows the comparison of $f''(0)$ ,$-\theta'(0)$ and $-\phi'(0)$ with those reported by M.S. Alam and M.M Rahman [31], which show a good agreement and we confident that our present numerical results are correct.

Table 2, and 3 shows the effects of Grashof number Gr, modified Grashof number Gc, Darcy number *Da,* magnetic parameter *M*, suction parameter $f_w$, Prandtl number *Pr*, radiation parameter *R*, heat generation parameter *Q*, Schmidt number *Sc* and chemical reaction parameter *Kr* on the physical parameters skin-friction coefficient $f''(0)$, Nusselt number $-\theta'(0)$ and Sherwood number $-\phi'(0)$ respectively. It can be seen that all of $f''(0)$, $-\theta'(0)$ and $-\phi'(0)$ increases as Grashof number *Gr*, modified Grashof number *Gc*, Darcy number *Da*, and suction parameter $f_w$ increases. $f'(0)$, $-\theta'(0)$ and $-\phi'(0)$ decreases as magnetic field parameter M increases. $-\theta'(0)$ increase as Prandtl number *Pr* or radiation parameter *R* increases, while it is decreases as heat generation parameter *Q* or Eckert number *Ec* increases. $-\phi'(0)$ increase as Schmidt number *Sc* or chemical reaction parameter *Kr* increases.

Finally, the effects of Soret number Sr and Dufour number Du on the skin-friction coefficient, Nusselt number and Sherwood number are shown in Table 4. The behavior of these parameters is self-evident from the Table 4 and hence they will not discuss any further due to brevity.

**Table 1 Comparison values of $f''(0), -\theta'(0)$ and $-\phi'(0)$ with different values of Soret and Dufour numbers.**

| *Sr* | *Du* | $f''(0)$ | | $-\theta'(0)$ | | $-\phi'(0)$ | |
|---|---|---|---|---|---|---|---|
| | | Alam and Rahman [31] | Present | Alam and Rahman [31] | Present | Alam and Rahman [31] | Present |
| 2.0 | 0.03 | 3.4231141 | 3.42938 | 1.0283189 | 1.02699 | 0.1296854 | 0.12749 |
| 1.0 | 0.06 | 3.3457474 | 3.35237 | 1.0155338 | 1.01386 | 0.2992750 | 0.297643 |
| 0.5 | 0.12 | 3.3162482 | 3.32295 | 1.0019868 | 1.00022 | 0.3844602 | 0.382995 |
| 0.4 | 0.15 | 3.3141130 | 3.32085 | 0.9965224 | 0.994735 | 0.4017999 | 0.400363 |
| 0.2 | 0.30 | 3.3287043 | 3.33558 | 0.9718535 | 0.969957 | 0.4381199 | 0.436742 |
| 0.1 | 0.60 | 3.3828661 | 3.38997 | 0.9248360 | 0.922756 | 0.4602605 | 0.458919 |

**Table 2: Numerical values of skin-friction coefficient ($Cf$), Nusseltl number $(Nu)$ and Sherwood number $(Sh)$ for, *Pr = 0.71, Fs = 1.0, Re = 100, R = 1.0, Du = 0.12, Sr = 0.5, Sc = 0.22, Ec = 0.1,Q = 1.0, Kr = 0.5.***

| *Gr* | *Gc* | *Da* | *M* | $f_w$ | $Cf$ | $Nu$ | $Sh$ |
|---|---|---|---|---|---|---|---|
| 12 | 6.0 | 1.0 | 1.0 | 0.5 | 6.34454 | 0.277773 | 0.921803 |
| 5 | 6.0 | 1.0 | 1.0 | 0.5 | 3.42049 | 0.287881 | 0.879048 |
| 10 | 6.0 | 1.0 | 1.0 | 0.5 | 5.54205 | 0.297256 | 0.910304 |
| 12 | 2.0 | 1.0 | 1.0 | 0.5 | 5.05881 | 0.288464 | 0.907465 |
| 12 | 4.0 | 1.0 | 1.0 | 0.5 | 5.70716 | 0.297754 | 0.914683 |
| 12 | 6.0 | 2.0 | 1.0 | 0.5 | 7.43037 | 0.246511 | 0.941017 |
| 12 | 6.0 | 3.0 | 1.0 | 0.5 | 7.90166 | 0.289481 | 0.949453 |
| 12 | 6.0 | 1.0 | 2.0 | 0.5 | 5.50345 | 0.295472 | 0.907287 |
| 12 | 6.0 | 1.0 | 3.0 | 0.5 | 4.76842 | 0.229296 | 0.894938 |
| 12 | 6.0 | 1.0 | 1.0 | 1.0 | 6.65476 | 0.307874 | 0.981984 |
| 12 | 6.0 | 1.0 | 1.0 | 2.0 | 7.12034 | 0.375616 | 1.10796 |

**Table 3: Numerical values of skin-friction coefficient ($Cf$), Nusseltl number $(Nu)$ and Sherwood number $(Sh)$ for *Gr = 12.0, Gc = 6.0, Da = 1.0, M = 1.0,* $f_w$ *= 0.5, Du = 0.12, Sr = 0.5***

| *Pr* | *R* | *Q* | *Ec* | *Sc* | *Kr* | $Cf$ | $Nu$ | $Sh$ |
|---|---|---|---|---|---|---|---|---|
| 0.71 | 1.0 | 1.0 | 0.1 | 0.22 | 0.5 | 6.34454 | 0.277773 | 0.921803 |
| 1.0 | 1.0 | 1.0 | 1.0 | 0.22 | 0.5 | 6.1504 | 0.355013 | 0.910383 |
| 1.5 | 1.0 | 1.0 | 0.1 | 0.22 | 0.5 | 5.8776 | 0.470762 | 0.893565 |
| 0.71 | 2.0 | 1.0 | 0.1 | 0.22 | 0.5 | 6.06827 | 0.34458 | 0.909912 |
| 0.71 | 3.0 | 1.0 | 0.1 | 0.22 | 0.5 | 5.90103 | 0.389547 | 0.902282 |
| 0.71 | 1.0 | 0.1 | 0.1 | 0.22 | 0.5 | 6.27499 | 0.366377 | 0.911571 |
| 0.71 | 1.0 | 0.5 | 0.1 | 0.22 | 0.5 | 6.3056 | 0.327556 | 0.916059 |
| 0.71 | 1.0 | 1.0 | 0.01 | 0.22 | 0.5 | 6.21768 | 0.34526 | 0.90238 |
| 0.71 | 1.0 | 1.0 | 0.05 | 0.22 | 0.5 | 6.32671 | 0.32516 | 0.91276 |
| 0.71 | 1.0 | 1.0 | 0.1 | 0.6 | 0.5 | 6.09895 | 0.277768 | 1.26436 |
| 0.71 | 1.0 | 1.0 | 0.1 | 0.78 | 0.5 | 6.01588 | 0.277751 | 1.41114 |
| 0.71 | 1.0 | 1.0 | 0.1 | 0.22 | 1.0 | 6.20678 | 0.276978 | 1.16894 |
| 0.71 | 1.0 | 1.0 | 0.1 | 0.22 | 2.0 | 6.02923 | 0.275442 | 1.54835 |

**Table 4: Numerical values of skin-friction coefficient ($Cf$), Nusseltl number $(Nu)$ and Sherwood number $(Sh)$ for, *Gr = 12.0, Gc = 6.0, Da = 1.0, M = 1.0,* $f_w$ *= 0.5, Du = 0.12, Sr = 0.5, , Pr = 0.71, Fs = 1.0, Re = 100, R = 1.0, Sc = 0.22, Q = 1.0 Ec = 0.1, Kr = 0.5.***

| *Sr* | *Du* | $Cf$ | $Nu$ | $Sh$ |
|---|---|---|---|---|
| 0.5 | 0.12 | 6.34454 | 0.277773 | 0.921803 |
| 1.0 | 0.12 | 6.35474 | 0.278037 | 0.920257 |
| 2.0 | 0.12 | 6.37527 | 0.278545 | 0.917239 |
| 0.5 | 0.03 | 6.3325 | 0.284933 | 0.920915 |
| 0.5 | 0.06 | 6.33651 | 0.282548 | 0.921211 |

## REFERENCES

[1] Nield DA, Bejan A , *2nd Edition, Springer-Verlag, Berlin*, **1998**.
[2] Hiremath PS, Patil PM , *Acta Mechanica*, **1993**, 98, 143-158.
[3] Sharma BK, Chaudhary RC, Sharma PK, *Advancesin Theoretical and Applied Mathematics*, **2007**, 2(3), 257-267
[4] Pop I, Ingham DB, *Pergamon*, Oxford, UK, **2001**.
[5] Ingham DB, Pop I, *Elsevier*, Oxford, **2005**.
[6] Vafai K , New York, NY,USA,2 edition, **2005**.
[7] Vadasz P, *Springer*, NewYork, **2008**.
[8] Gupta AS, *Appl.Sci.Res*., **1961**, 9(4), 319-333
[9] Lykoudis PS , *Int. J. Heat Mass Transfer*, **1962**, 5, 23-34.
[10] Nanda RS, Mohanty HK, *J. Phys.Soc. Japan*, **1970**, 29, 1608-1618.
[11] Chaudhary RC, Sharma BK , *Journal of Applied Physics*, **2006**, 99(3), 34901-34100.
[12] El-Amin MF, *Journal of Magnetism and Magnetic Materials*, **2001**, 234(3), 567-574.

[13] Raptis A, Kafoussias NG, *Can. J. Phys*., **1982**, 60(12), 1725–1729.
[14] Kim YJ, *Transport in Porous Media*, **2004**, 56(1), 17–37.
[15] Singh V, Shweta Agarwal (**2012**), *Int. J. of Appl. Math and Mech*., 2012, 8(4), 41-63.
[16] Makinde OD, Ogulu A, *Chemical Engineering Communications*, **2008**, 195(12), 1575-1584.
[17] Mohammed Ibrahim S, Sankar Reddy T, Bhaskar Reddy N, *Innovative Systems Design and Engineering*, **2013**, 4(13), pp. 76-88.
[18] Alharbi SM, Bazid MAA, El-Gendy MS, *Applied Mathematics*, **2010**, 1, 446-455.
[19] Gangadhar K, Bhaskar Reddy N, Kameswaran PK, *Int. J. Nonlinear Science*, **2012**, 13(3), 298-307.
[20] Ibrahim SY, Makinde OD, *Scientific Research and Essays*, **2010**, 5(19), 2875-2882.
[21] Eldabe NTM, Elsaka AG, Radwan AE , *Journal of American Science*, **2010**, 6(9), 126-136.
[22] Seddeek MA, Almushigeh AA, *Applications and Applied Mathematics*, **2010**, 5(1), 181-197.
[23] Mohammed Ibrahim S, *Advances in Applied Science Research*, **2013**, 4(1):371-382.
[24] Rajasekhar K., Ramana Reddy G V and Prasad B D C N, *Advances in Applied Science Research*, **2012**, 3(5), 2652-2659.
[25] Kishan N and Srinivas M, *Advances in Applied Science Research*, **2012**,3(1), 60-74.
[26] Anjali Devi S P and David A M G, *Advances in Applied Science Research*, **2012**, 3(1), 319-334.
[27] Vajravelu K, Hadjinicolaou A, *Int. Comm. Heat Mass Transfer*, **1993**, 20, 417-430.
[28] Hossain MA, Molla MM, Yaa LS, *Int. J.Thermal Science* , **2004**, 43, 157-163.
[29] Kesavaiah D Ch, Satyanarayana PV, Venkataramana S, *Int. J. of Appl. Math and Mech*., **2011**, 7(1), 52-69.
[30] Mohammed Ibrahim S, Bhaskar Reddy N, *Int. J. of Appl. Math and Mech*, **2011**, 8(8), 1-21.
[31] Anghel M, Takhar HS, Pop I, *Stud. Univ. Babes-Bolyai, Math*., **2000**, 45, 11-21.
[32] Postelnicu A, *Int. J. Heat Mass Transfer*, **2004**, 47, 1467–1472.
[33] M.S. Alam MS, M.M. Rahman MM, M.A. Maleque MA, M. Ferdows M, *Thammasat Int. J. Sci. Technol*., **2006**, 11(2), 1-12..
[34] Chamkha AJ, Ben-Nakhi A, *Heat Mass Transfer*, **2008**, 44, 845–856.
[35] Alam MS, Rahman MM, *J. Naval Architecture and Marine Engineering*, **2005**, 2(1), 55-65.
[36] Sreedhar Sarma G, Rama Krishna Prasad, Govardhan K, *IOSR Journal of Mathematics*, **2013**, 8(2), 67-87.
[37] Mansour MA, El-Anssary NF, Aly AM, *Journal of Chemical Engineering*, **2008**, 145(2), 340-345.
[38] El-Aziz MA, *Phys. Lett. A*, **2008**, 372, 263-272.
[39] Afify AA, *Commun. Nonlinear Sci. Numer. Simul*., **2009**, 14, 2204-2214.
[40] Alam MS, Ahammad MU, *Nonlinear Analysis: Modelling and Control*, **2011**, 16(1), 1-16.
[41] Sparrow EM, Cess RD, Augmented Edition, *Hemisphere Publishing Corp*, Washington, DC, **1978**.